Available online at www.sciencedirect.com
ScienceDirect
Journal of the Franklin Institute 344 (2007) 1075–1090
Journal of The Franklin Institute
www.elsevier.com/locate/jfranklin

Generalization of all stabilizing compensators for finite-dimensional linear systems

Yuan-Yong Huang, An-Chen Lee*

Department of Mechanical Engineering, National Chiao-Tung University, 1001 Ta-Hsueh Road, Hsinchu City, Taiwan, ROC

Received 3 September 2006; accepted 21 May 2007

Abstract

For finite-dimensional linear systems, the Youla–Kucera parameterization (YKP) with a Q parameter over RH_∞ is assumed to satisfy the Diophantine identity. However, the stability is guaranteed if the Diophantine equation is the "$\mathbf{U}(RH_\infty)$" equality, but not if it is the "identity" equality. However, Vidyasagar's structure with an H parameter over $\mathbf{U}(RH_\infty)$ is an observer–controller configuration that satisfies the Diophantine equation. This study discusses the deficiency of the Diophantine identity; expands the YKP using an H parameter over $\mathbf{U}(RH_\infty)$, and expands the Vidyasagar's structure using a Q_v parameter over RH_∞ so that both of the expanded parameterizations satisfy the Diophantine equation and are equivalent for all stabilizing compensators. Moreover, an equation that relates to Q, Q_v, and H will be introduced to establish relationships among the YKP, Vidyasagar's structure and both expanded parameterizations.

Keywords: Youla–Kucera parameterization; Diophantine equation; Diophantine identity; All stabilizing compensators

1. Introduction

All stabilizing controllers have to date involve well-known Youla–Kucera parameterization (YKP) with a Q parameter over RH_∞ for finite-dimensional linear systems [1–6]. The YKP is supposed to satisfy the Bezout identity or the Diophantine identity [3,6]. However, the stability is guaranteed when the Diophantine equation is the "$\mathbf{U}(RH_\infty)$"

*Corresponding author. Tel.: +886 3 5712121x55106; fax: +886 3 5725372.
E-mail address: aclee@mail.nctu.edu.tw (A.-C. Lee).

0016-0032/$32.00
doi:10.1016/j.jfranklin.2007.05.005

equality rather than the "identity" equality. The assumption of the Diophantine identity suggested by Youla et al. [3] causes the "$\mathbf{U}(RH_\infty)$" parameter to be omitted from the parameterization of all stabilizing compensators. The omission of the "$\mathbf{U}(RH_\infty)$" parameter makes finding another form of parameterization difficult. Vidyasagar [6] agreed that the YKP were all stabilizing compensators, and so included the stabilizing solutions to Vidyasagar's structure (VS) that he proposed. The VS with an H parameter over $\mathbf{U}(RH_\infty)$ is an observer–controller configuration that satisfies the Diophantine equation. However, the solutions to VS differ greatly from those to the YKP, as will be discussed herein. YKP and VS motivate the present study of the deficiency with the Diophantine identity, the expansion of the YKP (EYKP) by adding an H parameter over $\mathbf{U}(RH_\infty)$, and the expansion of VS (EVS) by adding a Q_v parameter over RH_∞ so that both of the expansions satisfy the Diophantine equation and are equivalent to all stabilizing compensators. Moreover, since H builds the bridge between the EYKP and the EVS, an equation in Q, Q_v, and H that connects YKP, VS, EYKP, and EVS can be introduced.

Other parameterizations of stabilizing controllers for other systems are available [7–11]. Infinite-dimensional linear systems [7,8], admit (weakly) left/right/ doubly coprime factorizations by means of Banach algebras; such systems which are algebraically and topologically more complex than the ring RH_∞. For structurally stable multidimensional systems, it is not known yet whether or not a stabilizable plant always has its doubly coprime factorization [9,10]; parameterization method of stabilizing controller without doubly coprime factorization is presented [11].

The study is laid out as follows. Section 2 discusses the deficiency of the Diophantine identity, which reduces the solutions to all stabilizing compensators. Moreover, the EYKP is introduced. Section 3 investigates VS again and develops the EVS. Moreover, the relationships among the EVS, VS, the EYKP, and the YKP are specified by an equation that relates Q, Q_v, and H. Section 4 presents an example that confirms the accuracy of the derivation and demonstrates the selection of Q, Q_v, and H and draws conclusions.

Mathematical notations:

$\mathbf{Re}(s)$	real part of s, where s is a complex variable
RH_∞	set of analytic real rational function matrices analytic in $\mathbf{Re}(s)>0$
$\boldsymbol{R}(s)$	set of real rational functions
$\boldsymbol{R}^{n\times n}$	consists of $n\times m$ matrices whose elements are in $\boldsymbol{R}(s)$
$H\in\boldsymbol{R}^{n\times n}$	unimodular matrix over RH_∞ if the inverse of H exists over RH_∞
$\mathbf{U}(RH_\infty)$	set of unimodular matrices over RH_∞
$\boldsymbol{R}_{\mathrm{p}}(s)$	set of proper rational transfer function matrices

2. The deficiency of diophantine identity

This section discusses the deficiency of the Diophantine identity, which the YKP satisfies, and elaborates an output-feedback controller and an observer–controller compensator with two independent parameters. One parameter is over RH_∞ and the other is over $\mathbf{U}(RH_\infty)$. Both of the compensators are input–output equivalent, and can be transformed into "the EYKP", which satisfies the Diophantine equation with an extra property that the YKP does not have.

The following well-known facts are presented as they will be extensively applied herein.

A system matrix $P(s)\in \boldsymbol{R}_{\mathrm{p}}(s)$ is said to exhibit doubly coprime factorization if there exists a right coprime factorization (rcf) of $P(s)$, i.e., $P = NM^{-1}$, a left coprime factorization (lcf) of $P(s)$, i.e., $P = \tilde{M}^{-1}\tilde{N}$, and X_{r}, Y_{r}, X_{l}, $Y_{\mathrm{l}}\in RH_{\infty}$ such that

$$\begin{bmatrix} X_{\mathrm{r}} & Y_{\mathrm{r}} \\ -\tilde{N} & \tilde{M} \end{bmatrix}\begin{bmatrix} M & -Y_{\mathrm{l}} \\ N & X_{\mathrm{l}} \end{bmatrix} = \begin{bmatrix} M & -Y_{\mathrm{l}} \\ N & X_{\mathrm{l}} \end{bmatrix}\begin{bmatrix} X_{\mathrm{r}} & Y_{\mathrm{r}} \\ -\tilde{N} & \tilde{M} \end{bmatrix} = I. \tag{1}$$

Then, the set of all negative output-feedback controllers achieving internal stability of $P(s)$ can be parameterized as follows:

$$C(s) = (X_{\mathrm{r}} + Q\tilde{N})^{-1}(Y_{\mathrm{r}} - Q\tilde{M}), \quad \det(I + Q\tilde{N}X_{\mathrm{r}}^{-1})(\infty)\neq 0, \tag{2}$$

$$C(s) = (Y_{\mathrm{l}} - MQ)(X_{\mathrm{l}} + NQ)^{-1}, \quad \det(I + X_{\mathrm{l}}^{-1}NQ)(\infty)\neq 0. \tag{3}$$

Eqs. (2) and (3) are the well-known YKP. Moreover, suppose $P(s)$ is controllable and observable, and its realization is

$$P = \left[\begin{array}{c|c} A & B \\ \hline C & D \end{array}\right], \tag{4}$$

where $A\in \boldsymbol{R}^{n\times n}$, $B\in \boldsymbol{R}^{n\times m}$, $C\in \boldsymbol{R}^{p\times n}$ and $D\in \boldsymbol{R}^{p\times m}$ are real constant matrices. Let F and L be such that $A+BF$ and $A+LC$ are both stable, then the coprime factor state models for the system and controller become

$$\left[\begin{array}{c:c} -M & Y_l \\ \hdashline N & X_l \end{array}\right] = \left[\begin{array}{c|c:c} A+BF & B & -L \\ \hline -F & -I & 0 \\ \hdashline C+DF & D & I \end{array}\right], \tag{5}$$

$$\left[\begin{array}{c:c} X_r & Y_r \\ \hdashline \tilde{N} & -\tilde{M} \end{array}\right] = \left[\begin{array}{c|c:c} A+LC & (B+LD) & -L \\ \hline -F & I & 0 \\ \hdashline C & D & -I \end{array}\right], \tag{6}$$

where $F\in \boldsymbol{R}^{m\times n}$ is a control gain matrix and $L\in \boldsymbol{R}^{n\times p}$ is an observer gain matrix [12]. However, the set of all stabilizing observer–controller compensators can be given by

$$y_{\mathrm{o}} = \bar{G}_u(s)u + \bar{G}_y y, \tag{7}$$

where y_{o} is the output of the observer–controller compensator and

$$\bar{G}_u(s) = X_{\mathrm{r}}(s) + Q(s)\tilde{N}(s) - I, \tag{8}$$

$$\bar{G}_y(s) = Y_{\mathrm{r}}(s) - Q(s)\tilde{M}(s). \tag{9}$$

The observer–controller compensator that is composed of $\bar{G}_u(s)$ and $\bar{G}_y(s)$ and the YKP are input–output equivalent because of $[I + \bar{G}_u(s)]^{-1}\bar{G}_y(s) = (X_{\mathrm{r}} + Q\tilde{N})^{-1}(Y_{\mathrm{r}} - Q\tilde{M})$.

The YKP given by Eq. (2) and the observer–controller compensator given by Eq. (7) are confined to the Diophantine identity as follows:

$$\begin{aligned}&[X_{\mathrm{r}}(s) + Q(s)\tilde{N}(s)]M(s) + [Y_{\mathrm{r}}(s) - Q(s)\tilde{M}(s)]N(s)\\ &\quad = [I + \bar{G}_u(s)]M + \bar{G}_y(s)N(s) = I.\end{aligned} \tag{10}$$

However, the internal stability is confirmed if the Diophantine equation is the "$\mathbf{U}(RH_\infty)$" equality [3,6]. The EYKP derived from the compensators in Theorem 1 or Corollary 2 below is utilized to demonstrate that for the EYKP, all stabilizing compensators satisfy the Diophantine equation, which is the "$\mathbf{U}(RH_\infty)$" equality.

Theorem 1. *The set of controllers in the following:*

$$C_1(s) = (HX_\mathrm{r} + W\tilde{N})^{-1}(HY_\mathrm{r} - W\tilde{M}) \tag{11}$$

are all stabilizing compensators and $H(s) \in \mathbf{U}(RH_\infty)$ *and* $W(s) \in RH_\infty$ *are independent of each other. As presented in Fig. 1* u_r *is the command reference,* u_d *is the input disturbance, and* u_n *is the sensor noise;* e_r, e_d, *and* e_n *are the internal signals, and* y *is the output of* $P(s)$.

Proof. Applying $X_\mathrm{r}(s)M(s) + Y_\mathrm{r}(s)N(s) = I$ and $\tilde{N}(s)M(s) - \tilde{M}(s)N(s) = 0$ to the left-hand side of Eq. (12) yields the right-hand side as follows:

$$(HX_\mathrm{r} + W\tilde{N})M + (HY_\mathrm{r} - W\tilde{M})N = H \in \mathbf{U}(RH_\infty). \tag{12}$$

Eq. (12) indicates that Eq. (11) satisfies the Diophantine equation. Also, Eq. (12) guarantees the internal stability of the system so that the nine transfer functions of Fig. 1 from (u_r, u_d, u_n) to $(e_\mathrm{r}, e_\mathrm{d}, e_\mathrm{n})$ are stable as follows:

$$\begin{bmatrix} e_\mathrm{r} \\ e_\mathrm{d} \\ e_\mathrm{n} \end{bmatrix} = \begin{bmatrix} MH^{-1} & MH^{-1}(HX_\mathrm{r} + W\tilde{N}) - I & -MH^{-1}(HY_\mathrm{r} - W\tilde{M}) \\ MH^{-1} & MH^{-1}(HX_\mathrm{r} + W\tilde{N}) & -MH^{-1}(HY_\mathrm{r} - W\tilde{M}) \\ NH^{-1} & NH^{-1}(HX_\mathrm{r} + W\tilde{N}) & I - NH^{-1}(HY_\mathrm{r} - W\tilde{M}) \end{bmatrix} \begin{bmatrix} u_\mathrm{r} \\ u_\mathrm{d} \\ u_\mathrm{n} \end{bmatrix}. \tag{13}$$

Hence, Eq. (11) describes all stabilizing compensators.

In Eq. (13), $H(s)$ appears in all nine elements, but $W(s)$ does not appear in the first column. Moreover, $W(s)$ and $H(s)$ have different characteristics. $H(s)$ must be invertible, but $W(s)$ need not be. $W(s)$ can have zeros in the right complex plane, but $H(s)$ cannot. Hence, $W(s)$ and $H(s)$ are mutually independent parameters. □

Since the feedback systems in Figs. 1 and 2 are input-output equivalent, the following Corollary 2 can be obtained directly from Theorem 1.

Corollary 2. *In Fig. 2, the set of observer–controller compensators is defined as follows:*

$$\bar{G}'_u(s) = H(s)X_\mathrm{r}(s) + W(s)\tilde{N}(s) - I, \tag{14}$$

$$\bar{G}'_y(s) = H(s)Y_\mathrm{r}(s) - W(s)\tilde{M}(s) \tag{15}$$

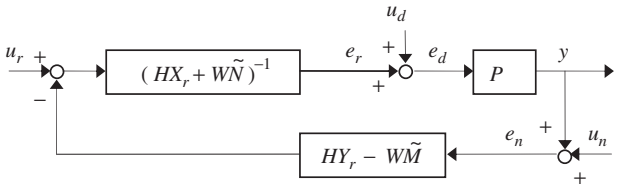

Fig. 1. Stabilizing controller in Theorem 1.

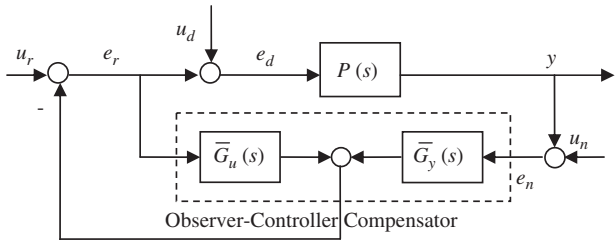

Fig. 2. Observer–controller configuration of Corollary 2.

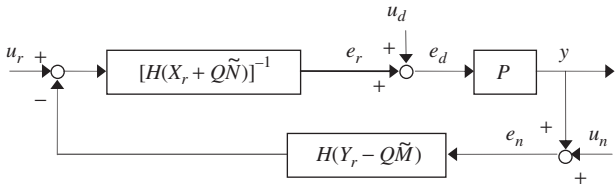

Fig. 3. Expansion of the Youla parameterization.

are all stabilizing compensators, and $H(s) \in \mathbf{U}(RH_\infty)$ *and* $W(s) \in RH_\infty$ *are independent of each other.*

In the feedback systems in Figs. 1 and 2, their compensators are equivalent for all stabilizing compensators that satisfy the Diophantine equation. If $W(s)$ is redefined as $H(s)Q(s)$, then the compensator of Fig. 1 can be redrawn as the EYKP in Fig. 3, where the nine transfer functions from (u_r, u_d, u_n) to (e_r, e_d, e_n) satisfy

$$\begin{bmatrix} e_r \\ e_d \\ e_n \end{bmatrix} = \begin{bmatrix} MH^{-1} & M(X_r + Q\tilde{N}) - I & -M(Y_r - Q\tilde{M}) \\ MH^{-1} & M(X_r + Q\tilde{N}) & -M(Y_r - Q\tilde{M}) \\ NH^{-1} & N(X_r + Q\tilde{N}) & I - N(Y_r - Q\tilde{M}) \end{bmatrix} \begin{bmatrix} u_r \\ u_d \\ u_n \end{bmatrix}. \tag{16}$$

In Eq. (16), $H(s)$ is eliminated from the second and third columns, but remains in the first column. That is, $H(s)$ in the EYKP exhibits the pre-filter property, but cannot contribute to feedback.

Notably, if $X_r(s) + Q(s)\tilde{N}(s)$ and $Y_r(s) - Q(s)\tilde{M}(s)$ are left coprime, then $H(s)[X_r(s) + Q(s)\tilde{N}(s)]$ and $H(s)[Y_r(s) - Q(s)\tilde{M}(s)]$ are also left coprime. This fact may explain the omission of the structure in Fig. 3 from all stabilizing controllers to date.

$H(s)$ in the EYKP that is related only to u_r, but not to u_d or u_n. The following section presents another equivalent parameterization of all stabilizing compensators, the EVS, where $H(s)$ relates to u_r, u_d, and u_n.

3. Vidyasagar's structure and all stabilizing compensators

VS is an observer–controller configuration, as displayed in Fig. 4 [6]. The observer that is composed of $X_r(s)$ and $Y_r(s)$ over RH_∞ reconstructs the "internal state" z as $\hat{z}$, and the controller $K(s) \in RH_\infty$ feeds back $\hat{z}$. The system is internally stable if and only if [6]

$$M(s) + K(s) = H(s) \in \mathbf{U}(RH_\infty). \tag{17}$$

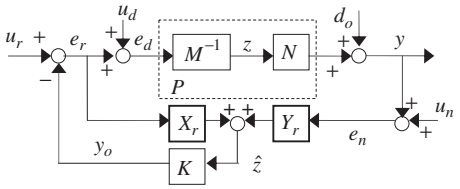

Fig. 4. Vidyasagar's structure (VS).

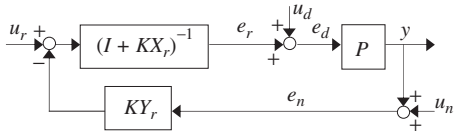

Fig. 5. Reduced block diagram of Fig. 4.

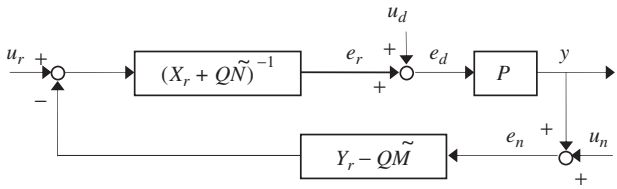

Fig. 6. Classical controller: the YKP.

Eq. (17) is derived from the Diophantine equation. The input–output equivalence is such that VS in Fig. 4 can be reduced to the compensator in Fig. 5 by reducing the block diagram. Vidyasagar [6] thought that the set of controllers in Fig. 5 was included in the set of controllers of Fig. 6, which is the YKP (Section 5.6 of [3].). However, comparing Eq. (17) with Eq. (10) raises a question about whether the configuration in Fig. 5 (or Fig. 4) differs from that in Fig. 6.

3.1. Another new parameterization, the common solution of VS and YKP, and of EVS and YKP, and the same solution of EVS and EYKP

In Fig. 7, the plant $P(s) \in \boldsymbol{R}_{\mathrm{P}}(s)$ has a rcf $(N(s), M(s))$ and a lcf $(\tilde{M}(s), \tilde{N}(s))$; $X_{\mathrm{r}}(s)$, $Y_{\mathrm{r}}(s) \in RH_\infty$ exist such that $X_{\mathrm{r}}(s)M(s) + Y_{\mathrm{r}}(s)N(s) = I$; $M(s)$ and $K(s)$ satisfy the equation $M(s) + K(s) = H(s) \in \mathbf{U}(RH_\infty)$; $Q_v(s) \in RH_\infty$. Before the relationship between VS and the YKP is clarified, another new parameterization in Fig. 7 must be demonstrated to involve all stabilizing compensators with two independent parameters: $Q_v \in RH_\infty$ and $H \in \mathbf{U}(RH_\infty)$ according to Theorem 3. Then, the condition under which the new parameterization and the EYKP have the same solutions can be obtained using Theorem 4. The new parameterization and the YKP have common solutions according to following Corollary 5 when the parameter H is the identity in both. The input–output equivalence enables the new parameterization of Fig. 7 to be unfolded to the EVS in Fig. 8, which becomes VS when Q_v is zero. Therefore, the common solution of the YKP and VS can be obtained directly from Corollary 5 by setting Q_v to be zero.

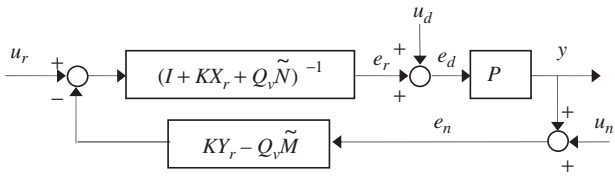

Fig. 7. Another new parameterization of all stabilizing compensators.

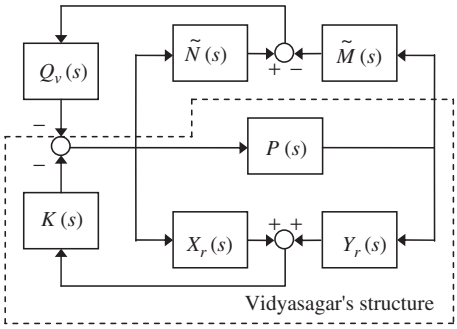

Fig. 8. Expansion of Vidyasagar's structure.

Theorem 3. (*i*) *For Fig. 7, the new parameterization*

$$C_{\mathrm{EVS}}(s) = [I + K(s)X_{\mathrm{r}}(s) + Q_v(s)\tilde{N}(s)]^{-1}[K(s)Y_{\mathrm{r}}(s) - Q_v(s)\tilde{M}(s)]$$
$$\det[I + K(s)X_{\mathrm{r}}(s) + Q_v(s)\tilde{N}(s)](\infty) \neq 0 \tag{18}$$

internally stabilizes the control system in Fig. 7 and (*ii*) *moreover,* $Q_v(s)$ *and* $H(s)$ *are mutually independent parameters.*

Proof. (i) For Fig. 7, the Diophantine equation

$$[I + KX_{\mathrm{r}} + Q_v\tilde{N}]M + [KY_{\mathrm{r}} - Q_v\tilde{M}]N = H \in \mathbf{U}(RH_\infty), \tag{19}$$

is satisfied by $\tilde{N}(s)M(s) - \tilde{M}(s)N(s) = 0$, $X_r(s)M(s) + Y_r(s)N(s) = I$, and $M(s) + K(s) = H(s)$ so that the nine transfer functions from $(u_{\mathrm{r}}, u_{\mathrm{d}}, u_{\mathrm{n}})$ to $(e_{\mathrm{r}}, e_{\mathrm{d}}, e_{\mathrm{n}})$

$$\begin{bmatrix} e_{\mathrm{r}} \\ e_{\mathrm{d}} \\ e_{\mathrm{n}} \end{bmatrix} = \begin{bmatrix} MH^{-1} & MH^{-1}(I + KX_{\mathrm{r}} + Q_{\mathrm{v}}\tilde{N}) - I & -MH^{-1}(KY_{\mathrm{r}} - Q_{\mathrm{v}}\tilde{M}) \\ MH^{-1} & MH^{-1}(I + KX_{\mathrm{r}} + Q_{\mathrm{v}}\tilde{N}) & -MH^{-1}(KY_{\mathrm{r}} - Q_{\mathrm{v}}\tilde{M}) \\ NH^{-1} & NH^{-1}(I + KX_{\mathrm{r}} + Q_{\mathrm{v}}\tilde{N}) & I - NH^{-1}(KY_{\mathrm{r}} - Q_{\mathrm{v}}\tilde{M}) \end{bmatrix} \begin{bmatrix} u_{\mathrm{r}} \\ u_{\mathrm{d}} \\ u_{\mathrm{n}} \end{bmatrix}, \tag{20}$$

are stable. Therefore, the feedback system in Fig. 7 is internally stable.

(ii) In Eq. (20), $H(s)$ is present in the nine elements, but $Q_v(s)$ does not appear in the first column. Moreover, $Q_v(s)$ and $H(s)$ have different characteristics. $H(s)$ must be invertible, but $Q_v(s)$ is not necessarily invertible. $Q_v(s)$ can have zeros in the right complex plane, but $H(s)$ cannot. Therefore, $Q_v(s)$ and $H(s)$ are independent parameters. □

Theorem 4. $N(s)$, $M(s)$, $\tilde{M}(s)$, $\tilde{N}(s)$, $X_{\mathrm{r}}(s)$, $Y_{\mathrm{r}}(s)$, $X_{\mathrm{l}}(s)$, *and* $Y_{\mathrm{l}}(s) \in RH_\infty$ *are doubly coprime satisfying Eq.* (*1*). *Then, the compensator in Fig. 7 and the EYKP in Fig. 3 have the same*

solutions if and only if the following equation is satisfied:

$$H(s)Q(s) = Y_1(s) + Q_v(s). \tag{21}$$

Proof. "if" $\Rightarrow$ Suppose $H(s)Q(s) = Y_1(s) + Q_v(s)$ is satisfied. Substituting the equation $M(s) + K(s) = H(s)$ and Eq. (21) into the compensator in Fig. 7, yields the following two equations:

$$KY_r - Q_v\tilde{M} = (H - M)Y_r - (HQ - Y_1)\tilde{M}(s), \tag{22}$$

$$I + KX_r + Q_v\tilde{N} = I + (H - M)X_r + (HQ - Y_1)\tilde{N}(s). \tag{23}$$

Applying $M(s)Y_r(s) = Y_1(s)\tilde{M}(s)$ by Eq. (1) to the right-hand side of Eq. (22), yields

$$KY_r - Q_v\tilde{M} = H(Y_r - Q\tilde{M}). \tag{24}$$

Applying $M(s)X_r(s) + Y_1(s)\tilde{N}(s) = I$ by Eq. (1) to the right-hand side of Eq. (23), yields

$$I + KX_r + Q_v\tilde{N}(s) = H(X_r + Q\tilde{N}). \tag{25}$$

Eqs. (24) and (25) reveal that the compensator in Fig. 7 is equivalent to the EYKP in Fig. 3 when Eq. (21) is satisfied. "only if" $\Rightarrow$ Suppose the compensator in Fig. 7 and the EYKP in Fig. 3 have the same solutions. Accordingly, one satisfies the following two equalities:

$$I + (KX_r + Q_v\tilde{N}) = H(X_r + Q\tilde{N}), \tag{26}$$

$$KY_r - Q_v\tilde{M} = H(Y_r - Q\tilde{M}). \tag{27}$$

Post-multiplying Eq. (26) by $Y_1(s)$, yields

$$Y_1 + (KX_r + Q_v\tilde{N})Y_1 = H(X_r + Q\tilde{N})Y_1. \tag{28}$$

Post-multiplying Eq. (28) by $X_1(s)$, yields

$$(KY_r - Q_v\tilde{M})X_1 = H(Y_r - Q\tilde{M})X_1. \tag{29}$$

Subtracting Eq. (29) from Eq. (28) yields (21) when $\tilde{N}(s)Y_1(s) + \tilde{M}(s)X_1(s) = I$, $X_r(s)Y_1(s) - Y_r(s)X_1(s) = 0$, according to Eq. (1). □

In Theorem 4, if the new parameterization of Eq. (18) satisfies Eq. (21) and is expressed as displayed in Fig. 7, then the new parameterization of Eq. (18) provides the same solutions as the EYKP in Fig. 3. When $H(s)$ is an identity within the new parameterization and the EYKP, $K(s)$ in Eq. (18) satisfies the equation $K(s) = I - M(s)$, and the EYKP becomes the YKP. Therefore, the condition under which the compensators in Figs. 6 and 7 have common solutions is presented in Corollary 5 as follows.

Corollary 5. *The compensators in Figs. 6 and 7 have common solutions when the following equations are satisfied*

$$K(s) = I - M(s), \tag{30}$$

$$Q(s) = Y_1(s) + Q_v(s). \tag{31}$$

Proof. By Theorem 4 and the above description.

When $Q_v(s)$ is zero, the control system in Fig. 7 becomes the control system in Fig. 5. Also, the compensator in Fig. 5 is equivalent to VS. Clearly by Corollary 5, VS and the YKP have a common solution when the two equations: $K(s) = I - M(s)$ and $Q(s) = Y_1(s)$ are satisfied. That is, VS in Fig. 4 and the YKP in Fig. 6 have only one common solution when $H(s)$ is the identity and $Q(s) = Y_1(s)$. When $H(s)$ is not the identity, the solutions to VS in Fig. 4 are different from the ones to the YKP in Fig. 6. □

3.2. Mapping relationships among the EYKP, the YKP, the EVS, and VS

The EVS has the same solutions as the EYKP. That is, $H(s)$, $Q(s)$, and $Q_v(s)$ satisfy $H(s)Q(s) = Q_v(s) + Y_1(s)$ so that each solution in both EVS and EYKP can be can mapped onto each other. Here, $H(s)$ bridges them. While each solution in the EVS corresponds to an $H(s) \in \mathbf{U}(RH_\infty)$ and a $Q_v(s) \in RH_\infty$, each solution in the EYKP corresponds to an $H(s) \in \mathbf{U}(RH_\infty)$ and a $Q(s) \in RH_\infty$. When $H(s)$ is an identity, the EYKP reduces to the YKP, and the common solutions between the YKP and the EVS satisfy $Q(s) = Y_1(s) + Q_v(s)$. When $Q_v(s)$ is zero, the EVS reduces to VS, and the common solutions of VS and the EYKP satisfy the equality $H(s)Q(s) = Y_1(s)$. Therefore, VS and the YKP have a single solution when $H(s)$ is the identity, $Q_v(s)$ is zero, and $Q(s) = Y_1(s)$. Fig. 9 presents the mappings among the EVS, VS, the EYKP, and the YKP.

Although $H(s)$ bridges the EVS and the EYKP, it plays a different role in each. By Eq. (20), $H(s)$ in the EVS has the feedback property that is related to u_d and u_n and the pre-filter property that relates to u_r. By Eq. (16), H(s) in the EYKP exhibits only the pre-filter property that relates to u_r. $Q_v(s)$ of the EVS and $Q(s)$ of the EYKP exhibit have the feedback property that relates to u_d and u_n.

4. An example and conclusion

An example of equivalent mappings within the EVS and the EYKP is presented, indicating the selection of Q, Q_v, and H to improve performance. Conclusions are then drawn.

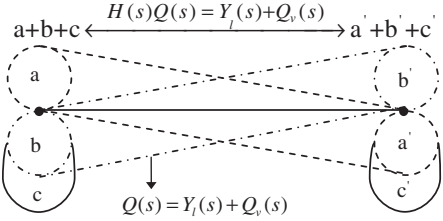

The EVS(a+b+c), VS(a), The EYKP(a'+b'+c'), The YKP(b')

a: $\{Q_v(s), H(s) \mid Q_v(s) = 0\}$ a': $\{Q(s), H(s) \mid Q(s) = H^{-1}(s)Y_l(s)\}$

b: $\{Q_v(s), H(s) \mid H(s) = I\}$ b': $\{Q(s), H(s) \mid H(s) = I\}$

c: $\{Q_v(s), H(s) \mid Q_v(s) \neq 0, H(s) \neq I\}$ c': $\{Q(s), H(s) \mid Q(s) \neq H^{-1}(s)Y_l(s), H(s) \neq I\}$

Fig. 9. Mappings among the EVS, VS, the EYKP, and the YKP.

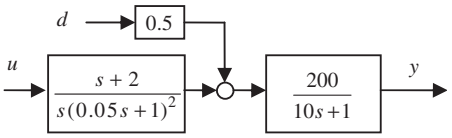

Fig. 10. Block diagram representation of the plant and its disturbance.

Example 1. (The sample is adapted from example 9.3 in [13], pp. 381.) The nominal plant $P(s)$ and its disturbance dynamics $P_d(s)$ are considered as follows:

$$P(s) = \frac{200}{10s+1}\,\frac{s+2}{s(0.05s+1)^2}, \quad P_d(s) = \frac{100}{10s+1}. \tag{32}$$

The plant and its disturbance d are represented by the block diagram in Fig. 10. The disturbance enters at the plant input in the sense that $P(s)$ and $P_d(s)$ share the same dominating dynamics, which are represented by the term $200/(10s+1)$. $\tilde{M}(s)$, $\tilde{N}(s)$, $M(s)$, $X_r(s)$, $Y_r(s)$, and $Y_l(s)$ are given by

$$\tilde{N}(s) = \frac{8000s + 16\,000}{s^4 + 54.87s^3 + 1105s^2 + 9969s + 16\,000}, \tag{33}$$

$$\tilde{M}(s) = \frac{s^4 + 40.1s^3 + 404s^2 + 40s}{s^4 + 54.87s^3 + 1105s^2 + 9969s + 16\,000}, \tag{34}$$

$$N(s) = \frac{8000s + 16\,000}{s^4 + 112.1s^3 4046s^2 + 61\,280s + 103\,900}, \tag{35}$$

$$M(s) = \frac{s^4 + 40.1s^3 + 404s^2 + 40s}{s^4 + 112.1s^3 + 4046s^2 + 61\,280s + 103\,900}, \tag{36}$$

$$X_r(s) = \frac{s^4 + 126.8s^3 + 5810s^2 + 132\,900s + 243\,300}{s^4 + 54.87s^3 + 1105s^2 + 9969s + 16\,000}, \tag{37}$$

$$Y_r(s) = \frac{143.6s^3 + 6201s^2 + 73\,450s + 103\,900}{s^4 + 54.87s^3 + 1105s^2 + 9969s + 16\,000}, \tag{38}$$

$$Y_l(s) = \frac{143.6s^3 + 6201s^2 + 73\,450s + 103\,900}{s^4 + 112.1s^3 + 4046s^2 + 61\,280s + 103\,900}. \tag{39}$$

According to Eqs. (37) and (38), the central controller $X_r^{-1}(s)Y_r(s)$ for the YKP performs well when d is a unit step function, as presented in Figs. 11 and 12. Next, a compensator in EVS and a compensator in the YKP must be found such that the final value y equals zero when d is a sinusoidal signal, $\sin t$.

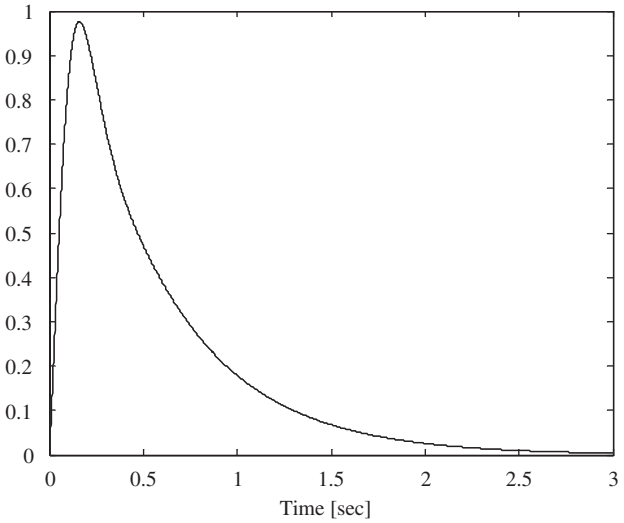

Fig. 11. Unit-step disturbance response.

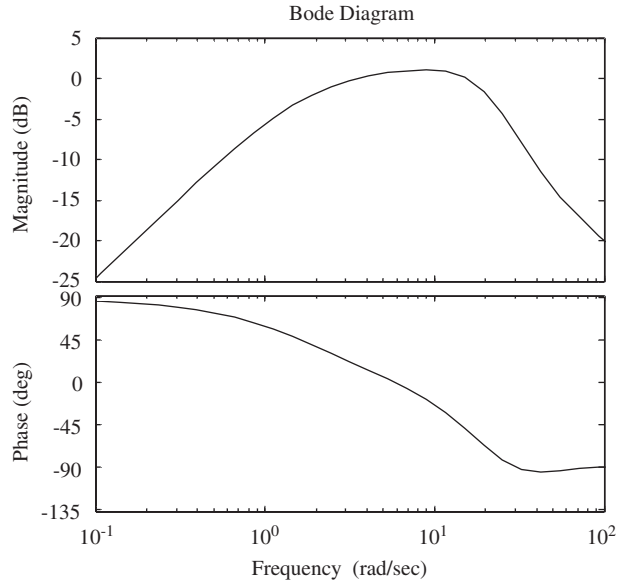

Fig. 12. Transfer function from d to y.

Firstly, an approach proposed elsewhere [14] is adopted to obtain a proper $C(s)$ in the form of Eq. (2). For such $C(s)$, the transfer function from d to y is $100/(10s+1)$ $M(s)[X_r(s)+Q_1(s)\ \tilde{N}(s)]$, where $Q_1(s)$ is the first estimate of the parameter $Q(s)$. The sinusoid d is rejected if

$$100/(10j+1)M(1j)[X_r(1j)+Q_1(1j)\tilde{N}(1j)]=0. \tag{40}$$

Hence, the problem reduces to the purely algebraic problem of finding $Q_1(s) \in RH_\infty$ that satisfies Eq. (40), which reduces to

$$Q_1(1j) = -15.194 - 0.701j. \tag{41}$$

Eq. (41) can be written as two equations

$$\mathrm{Re}\, Q_1(1j) = -15.194, \tag{42}$$

$$\mathrm{Im}\, Q_1(1j) = -0.701. \tag{43}$$

Hence, a parameter $Q_1(s) \in RH_\infty$ that satisfies Eqs. (42) and (43) must be found. An effective method is to let $Q_1(s)$ be a polynomial in $(s+9)^{-1}$ with sufficient variable coefficients, guaranteeing that $Q_1(s) \in RH_\infty$. Since two equations must be satisfied, two coefficients are allowed. $Q_1(s)$ is of the form

$$Q_1(s) = c_1 + \frac{c_2}{s+9}. \tag{44}$$

The two Eqs. (42) and (43) yield one of the form $Ac = b$, where $c = [c_1' \quad c_2']'$. This equation is solved for c. In this case, the solution is

$$c_1 = -21.62, \quad c_2 = 58.417.$$

These values give

$$Q_1(s) = \frac{-21.62s - 136.163}{s+9}. \tag{45}$$

Hence, from Eqs. (33), (34), (37), (38), and (45), $C(s)$ is obtained as follows:

$$C(s) = \frac{\begin{array}{c}21.62s^9 + 2333s^8 + 1.085\times10^5 s^7 + 2.858\times10^6 s^6 + 4.668\times10^7 s^5 \\ 4.824\times10^8 s^4 + 3.095\times10^9 s^3 + 1.168\times10^{10} s^2 + 2.165\times10^{10} s + 1.496\times10^{10}\end{array}}{\begin{array}{c}s^9 + 190.7s^8 + 1.551\times10^4 s^7 + 5.538\times10^5 s^6 + 9.728\times10^6 s^5 \\ 8.516\times10^7 s^4 + 2.374\times10^8 s^3 + 2.445\times10^8 s^2 + 1.7\times10^8 s + 1.767\times10^8\end{array}}. \tag{46}$$

With the value of $C(s)$ given by Eq. (46), the Bode plot of the closed loop transfer function from d to y is presented in curve 1 in Fig. 13.

Secondly, a proper $C_{\mathrm{EVS}}(s)$ from Eq. (18) must be found and outperforms $C(s)$ in Eq. (46). If $H_1(s)$ is the first estimate of the parameter $H(s)$, then $H_1(s)$ causes the point A $\{Q_1(s), I\}$ in the YKP to move to the point B $\{Q_1(s), H_1(s)\}$ in the EYKP, as presented in Fig. 14. $H_1(s)$ is arbitrarily set to

$$H_1(s) = \frac{21s + 136}{21.62s + 136.163} \tag{47}$$

since $H_1(s)$ is not related to d for the EYKP. Moreover, $H_1(s)$ provides the bridge to map the point B $\{Q_1(s), H_1(s)\}$ onto the corresponding point C $\{Q_{v1}(s), H_1(s)\}$ in the EVS, as presented in Fig. 14. $Q_{v1}(s)$ is given by

$$\begin{aligned} Q_{v1}(s) &= H_1(s)Q_1(s) - [Y_l(s) \text{ of (39)}] \\ &= \frac{-21s^5 - 2633s^4 - 1.077\times10^5 s^3 - 1.966\times10^6 s^2 - 1.128\times10^7 s - 1.506\times10^7}{s^5 + 121.1s^4 + 5054s^3 + 9.769\times10^4 s^2 + 6.554\times10^5 s + 9.349\times10^5}. \end{aligned} \tag{48}$$

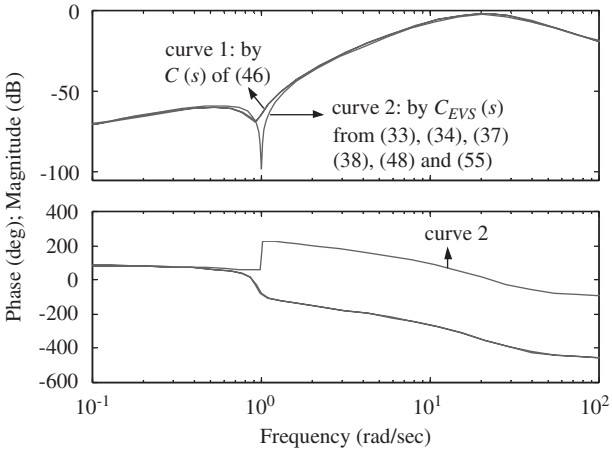

Fig. 13. Bode plots of the transfer functions from d to y.

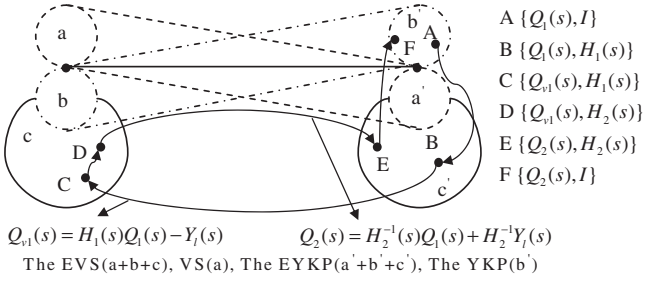

Fig. 14. Mappings in this example.

Since the points A, the point B, and the point C perform equally for d, another $H_2(s)$ is sought to replace $H_1(s)$ to improve the performance of d in the EVS, where $H_2(s)$ is the second estimate of the parameter $H(s)$. The sinusoid d is rejected if

$$100/(10j+1)M(1j)H_2(1j)^{-1}[1 + (H_2(1j) - M(1j))X_r(1j) + Q_{v1}(1j)\tilde{N}(1j)] = 0. \quad (49)$$

The problem reduces to the purely algebraic problem of finding $H_2(s) \in RH_\infty$ that satisfies Eq. (49), which in turn reduces to

$$H_2(1j) = 0.999 - 0.0035j. \quad (50)$$

Eq. (50) can be expressed as two equations

$$\mathrm{Re}\, H_2(1j) = 0.999, \quad (51)$$

$$\mathrm{Im}\, H_2(1j) = -0.0035. \quad (52)$$

A parameter $H_2(s) \in \mathbf{U}(RH_\infty)$ that satisfies Eqs. (51) and (52) must be found. Since two equations must be satisfied, two coefficients are required. $H_2(s)$ is of the form

$$H_2(s) = \frac{k_1(s+k_2)^2}{(s+100)^2}. \quad (53)$$

If $k_2 > 0$ then Eq. (53) guarantees that $H_2(s) \in \mathbf{U}(RH_\infty)$. The two Eqs. (51) and (52) yield one of the form

$$\begin{bmatrix} 10^{-4} & 4\times 10^{-6} \\ -2\times 10^{-6} & 1.999\times 10^{-4} \end{bmatrix} \begin{bmatrix} k_1(k_2^2-1) \\ k_1 k_2 \end{bmatrix} = \begin{bmatrix} 9.99\times 10^{-1} \\ -3.5\times 10^{-3} \end{bmatrix}. \tag{54}$$

The solution to Eq. (54) is

$$k_1 = 6.796\times 10^{-1}, \quad k_2 = 121.2425,\ -8.2\times 10^{-3}.$$

These values give

$$H_2(s) = 6.796\times 10^{-1}\frac{(s+121.2425)^2}{(s+100)^2}. \tag{55}$$

With $H_2(s)$ and $Q_{v1}(s)$ the solution in the EVS moves from the point C to the point D in Fig. 14. From Eqs. (33), (34), (37), (38), (48), and (55), $C_{\mathrm{EVS}}(s)$ can be obtained. Curve 2 in Fig. 13 is the Bode plot of the closed loop transfer function from d to y for such $C_{\mathrm{EVS}}(s)$. From Fig. 15, $C_{\mathrm{EVS}}(s)$ with Q_{v1} and H_2 rejects the sinusoidal signal d almost completely and exhibits less transient oscillation than does $C(s)$ with Q_1.

From Fig. 14, one sees that $H_2(s)$ provides the bridge to map the point D $\{Q_{v1}(s), H_2(s)\}$ onto the point E $\{Q_2(s), H_2(s)\}$ where

$$\begin{aligned} Q_2(s) &= H_2^{-1}(s)Q_{v1}(s) + H_2^{-1}Y_1(s) \\ &= 1.4715\times \frac{(s+100)^2}{(s+121.2425)^2}\frac{-21s-136}{s+9}, \end{aligned} \tag{56}$$

which is the second estimate of the parameter $Q(s)$. Since $H_2(s)$ in the EYKP is unrelated to d, the points E and F $\{Q_2(s), I\}$ in Fig. 14 perform similarly for d. $Q_2(s)$ in Eq. (56) yields a controller in the YKP such that the Bode plot for the closed loop transfer function from d to y is curve 2 in Fig. 13. Thus, $Q_2(s)$ in Eq. (56) outperforms $Q_1(s)$ in Eq. (45).

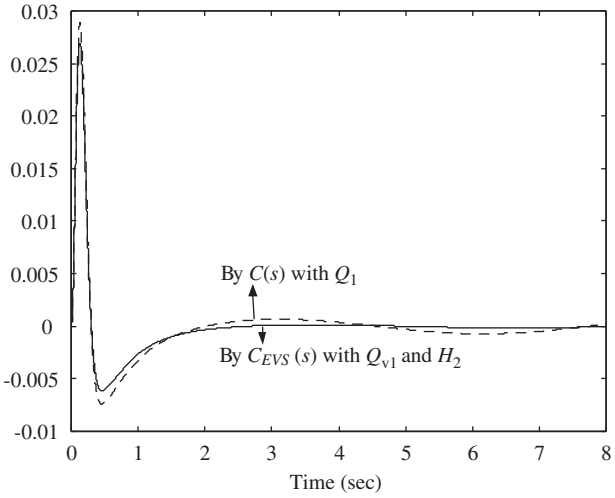

Fig. 15. Responses from d to y for $d = \sin t$ by using C and C_{EVS}.

In conclusion, the EVS and the EYKP are equivalent to all stabilizing compensators for finite-dimensional linear systems. Given $H(s)$, the solutions to both can be mapped onto each others and the mapping relationships are explained by the equation, $HQ = Y_1 + Q_v$. $H(s)$ in the EYKP exhibits the pre-filter property, but $H(s)$ in EVS exhibits the properties of pre-filter and feedback. Q of the EYKP and Q_v of the EVS exhibit the feedback property. The equation yields the relationships among the EYKP, the YKP, the EVS, and VS. In particular, VS and the YKP have only a single common solution. Moreover, the example illustrates the selection of Q, Q_v, and H to improve performance.

The parameterization is well known to increase the orders of the compensator. Frequency-weighted extensions of three basic methods are employed to solve controller reduction problems. The approaches are balanced truncation approximation (BTA), singular perturbation approximation (SPA) and Hankel-norm approximation (HNA) can be employed. Theoretical and computational enhancements of the frequency-weighted BTA and SPA methods have been proposed elsewhere [15,16]. They have been extended to solve efficiently a class of stability/performance preserving controller reduction problems [16,17], the stability-preserving frequency-weighted coprime factor controller reduction problem [18], and the performance-preserving frequency-weighted coprime factor H_∞ controller reduction problem [19].

In the future work, one will propose a design procedure and guide lines for selecting H and Q_v to improve the performance of the EVS.

Acknowledgement

This study was supported by the National Science Council, Republic of China, under Contract number NSC 93-2212-E-009-002.

References

[1] V. Kucera, Stability of discrete linear feedback systems, in: Proceedings of the IFAC World Congress, Boston, MA. Paper No. 44-1, 1975.
[2] V. Kucera, Discrete Linear Control: The Polynomial Equation Approach, Wiley, New York, 1979.
[3] D.C. Youla, H.A. Jabr, J.J. Bongiorno Jr., Modern Wiener–Hopf design of optimal controllers—part II: the multivariable case, IEEE Trans. Automat. Control 21 (1976) 319–338.
[4] C.A. Desoer, R.W. Liu, J. Murray, R. Saeks, Feedback system design: the fractional approach to analysis and synthesis, IEEE Trans. Automat. Control 25 (1980) 399–412.
[5] P.J. Antsaklis, M.K. Sain, Unity feedback compensation of unstable plants, in: Proceedings of the 20th IEEE Conference on Decision and Control, San Diego, December 1981, pp. 305–308.
[6] M. Vidyasagar, Control System Synthesis, MIT Press, Cambridge, MA, 1985.
[7] A. Quadrat, The fractional representation approach to synthesis problems: an algebraic analysis viewpoint part I: (weakly) doubly coprime factorizations, SIAM J. Control Optim. 42 (1) (2003) 266–299.
[8] A. Quadrat, The fractional representation approach to synthesis problems: an algebraic analysis viewpoint part II: internal stabilization, SIAM J. Control Optim. 42 (1) (2003) 300–320.
[9] Z. Lin, Output feedback stability and stabilization of linear n-D systems, in: Multidimensional Signals, Circuits and Systems, Taylor & Francis, New York, NY, 2001.
[10] Z. Lin, Feedback stabilization of MIMO 3-D linear systems, IEEE Trans. Automat. Control 44 (1999) 1950–1955.
[11] K. Mori, A new parameterization method for all stabilizing controllers of nD systems without coprime factorizability, IEEE Trans. Automat. Control III (2003) 678–681.
[12] K. Zhou, J.C. Doyle, Essentials of Robust Control, Prentice-Hall, Englewood Cliffs, 1998.

[13] S. Skogestad, I. Postlethwaite, Multivariable Feedback Control: Analysis and Design, Wiley, New York, 1996.
[14] J.C. Doyle, B.A. Francis, A.R. Tannenbaum, Feeback Control Theory, Macmillan Publishing Co., New York, 1992.
[15] A. Vagra, D.D.O. Anderson, Square-root balancing-free methods for the frequency-weight balancing related model reduction, in: Proceedings of CDC '2001, Orlando, Florida, 2001.
[16] A. Vagra, D.D.O. Anderson, Accuracy-enhancing methods for balancing- related frequency-weighted model and controller reduction, Automatica 39 (2003) 919–927.
[17] A. Vagra, D.D.O. Anderson, Frequency-weighted balancing related controller reduction, in: Proceedings of IFAC Congress, Barcelona, Spain, 2002.
[18] A. Vagra, On frequency-weighted coprime factorization based controller reduction, in: Proceedings of ACC, Denver, CO, 2003.
[19] A. Vagra, Coprime factor reduction of H-infinity controller, in: Proceedings of ECC, Cambridge, UK, 2003.